
Proceedings Paper:
Yan, Jiexiong, Dawson, John orcid.org/0000-0003-4537-9977 and Marvin, Andy orcid.org/0000-0003-2590-5335 (2017) Effect of power state on absorption cross section of personal computer components. In: 2017 International Symposium on Electromagnetic Compatibility - EMC EUROPE. EMC Europe 2017, 04-08 Sep 2017 , FRA.

https://doi.org/10.1109/EMCEurope.2017.8094782

2017 International Symposium on Electromagnetic Compatibility - EMC EUROPE , 4-8 September, 2017

Effect of power state on absorption cross section of personal computer components

Applications to enclosure shielding

Jiexiong Yan, John Dawson, and Andy Marvin
Department of Electronics
University of York
York, UK
{jy936, john.dawson, andy.marvin}@york.ac.uk

***Abstract*—Knowledge of the shielding effectiveness of an enclosure is important for the electromagnetic compatibility of electronic systems. The shielding effectiveness of an enclosure depends on the absorption cross section of its contents. It might be expected that the energy absorption in an electronic circuit changes according to the operating state of the semiconductor devices which compose the active components. In most published research, the absorption cross section measurements were performed when the contents were unpowered. In this paper we compare the measured absorption cross sections of the components of a personal computer in powered and unpowered states. Comparisons indicate that power and the particular operating configuration do not have a significant influence on the absorption cross section. This means that the process of determining absorption cross sections of circuit boards and other components can be easily achieved without the need to provide power and define a particular operating state.**

Keywords— shielding effectiveness; aborption cross section; reverberation chamber

I. INTRODUCTION

The ability of an electronic device's enclosure to protect the device against electromagnetic interference is quantified by its shielding effectiveness (SE). Existing standards such as IEEE 299.1 [1] specify the measurement of the SE of an empty enclosure. In real applications, an enclosure is used with some contents inside it. Previous work has shown that contents can affect the SE of an enclosure [2]-[5] since they absorb some energy and thus decrease the internal field. To accurately predict the shielding effectiveness of populated enclosures, it is necessary to understand these effects.

One successful approach to analyze the shielding problems of electrically large enclosures with contents is the power balance method (PWB) proposed by Hill et al [6]. The main advantages of the method are that it does not require the knowledge of the detailed geometry of contents and it has a low computational cost compared with full wave solvers. In order to apply the power balance method, the contents are characterized by their absorption cross sections (ACSs); and the apertures of the enclosure are characterized by their transmission cross sections (TCSs). The ACS, σ_a (m^2), of an object is the equal to the area of a perfect absorber that would absorb the same amount of energy. It is defined as the ratio of the absorbed power (W) to the incident power density (W/m^2). The TCS, σ_t (m^2), of an aperture is an area equal to the ratio of the power transmitted through the aperture (W) to the incident power density (W/m^2). The SE of an electrically large enclosure in a reverberant environment may be defined as the ratio of external (incident) energy density (S_o) to the internal energy density (S_i) and can be expressed directly in terms of the ACS of the contents and TCS of any apertures [7]:

$$SE = \frac{S_o}{S_i} = \frac{\sigma_t + \sigma_a}{\sigma_t} \quad (1)$$

where the ACS and TCS are assumed to be values averaged over all angles of incidence.

In previous research, the ACSs of printed circuit boards (PCBs) have been measured in a reverberation chamber [5]-[8] and the measurements were performed when the PCBs were unpowered. We expected that the power state (power on or power off) might affect the ACS of electronic equipment as the active devices in the circuit tend to be non-conducting when powered off and conducting only when powered on. Consider a digital circuit that contains a logic gate. When the circuit is not powered, the transistors of the logic gate are non-conducting, whereas when the circuit is powered, some of the transistors are switched into conduction to determine the logic state of the gate; this changes the circuit impedance and hence we would expect a change in power absorbed from an external field. We would also expect the impedance of the circuit to change as the logic gate changes state. We have observed this in the re-radiated energy from digital systems [9]. To test our assumption, in this work we measured the ACS of the internal components of a personal computer, in both powered and unpowered states in a reverberation chamber.

978-1-5386-0689-6/17/$31.00 ©2017 IEEE

(a) (b) (c)

Fig. 1. Photos of the computer under test. (a) Side view (without side panel). (b) Front view (without cover). (c) Rear view.

Section II provides the details of the computer. Section III outlines the theory of ACS measurement. Section IV presents the measurement results and section V is the conclusion.

II. Computer Under Test

Figure 1 shows the personal computer under test which has dimensions of 370mm×180mm×350mm. It can be seen that there are various apertures of different shapes and sizes in the enclosure. Inside the computer there are a motherboard, a power supply unit, a CD-ROM, a disk drive, several wires and some extra structures. During the measurements the keyboard, mouse and monitor of the computer were removed. Also, the side panel of the computer was removed to expose the circuitry to the electromagnetic energy in the chamber thus enabling the overall ACS to be measured.

III. Measurement Of ACS

A. Measurement Methodology

The ACS measurements were performed in a reverberation chamber with dimensions of 4.7m×3m×2.37m and a lowest useable frequency (at three times the first resonance) of approximately 178MHz. The cross over frequency, or the Schroeder frequency of the empty chamber, at which the ratio of mode bandwidth and mode spacing is 3, is about 1.7GHz. A mechanical stirrer was fitted into the chamber to achieve field homogeneity. The diagram of the measurement configuration is shown in Figure 2. Two Blade antennas were used for the measurements and their details can be found in [11]. A vector network analyzer was used to collect *S*-parameters from the two antennas.

Figure 3 is a photo of the measurement set up. The antennas were placed at two opposite corners of the chamber. To reduce the coupling, they were not facing each other. The computer was supported on a polystyrene block. The antennas and the computer were at least 0.2m away from the chamber walls and the floor. This guarantees that they are at least a quarter wavelength away from the chamber

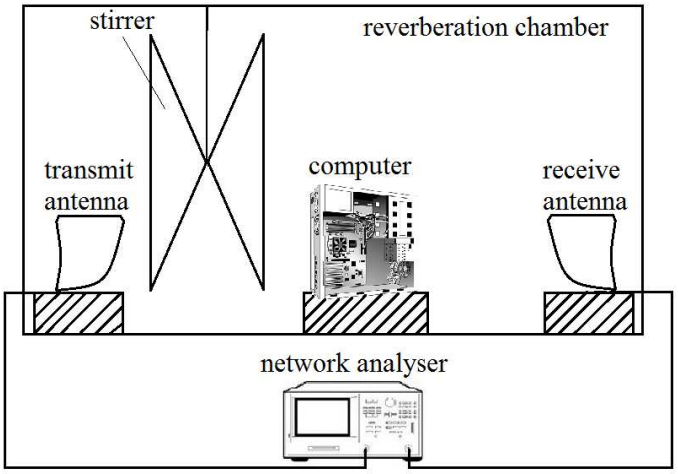

Fig. 2. Diagram of the reverberation chamber set up for the ACS measurements.

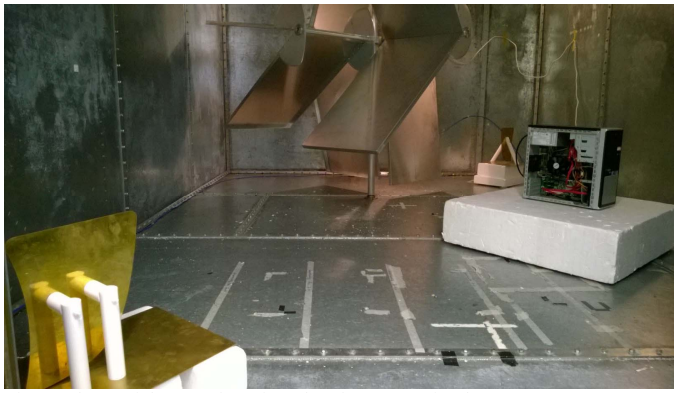

Fig. 3. Photo of the reverberation chamber set up for the ACS measurements.

over the whole frequency range used.

B. Frequency domain method

Initially we followed the method described in [8] where the average ACS of an object in a reverberation chamber is given by:

$$\langle \sigma_a \rangle = \frac{\lambda^2}{8\pi}\left(\frac{1}{\langle G_{wo} \rangle} - \frac{1}{\langle G_{no} \rangle}\right) \qquad (2)$$

where $\langle\ \rangle$ indicates an average over a number of measurements with either different stirrer positions and/or over a range of frequencies; λ is the wavelength; $\langle G_{wo} \rangle$ and $\langle G_{no} \rangle$ are the measured average net power transfer function between antennas in the chamber with and without the object respectively. The net power transfer function is obtained by:

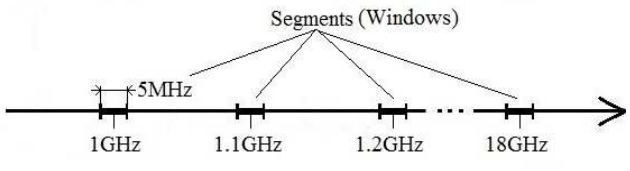

Fig. 4. Diagram of the distribution of the frequency segments for the time domain method.

$$\langle G \rangle = \frac{\langle |S_{21}|^2 \rangle}{\left(1 - |\langle S_{11} \rangle|^2\right)\left(1 - |\langle S_{22} \rangle|^2\right)} \quad (3)$$

where S_{21} is the transmission coefficient between the transmitting and receiving antennas, S_{11} and S_{22} are the reflection coefficients of the two antennas. The losses within each antenna are assumed to be negligible.

The measurement uncertainty is defined as:

$$\alpha = \frac{std(\sigma_a)}{\sigma_a} \quad (4)$$

where $std(\sigma_a)$ is the standard deviation of the ACS over a number of measurements with either different stirrer positions and/or over a range of frequencies. In [10], Flintoft et al include a model to calculate the uncertainty of ACS measurements in a reverberation chamber. Both (4) and the method in [10] led to similar uncertainty, which is about 20%.

The ACS of the computer was measured from 1GHz to 18GHz. For the frequency domain method, the mechanical stirrer was set to move 100 uniformly spaced positions over one rotation. 10001 equal-spaced points were recorded over the frequency range. The sweep time of the network analyzer was 4s. The frequency stirring technique, using a bandwidth of 100MHz, was applied to the measured data to further reduce measurement error.

C. Time domain method

A measurement uncertainty of 20% was considered too high to allow small changes to ACS to be observed. Therefore, we also measured the ACS of the computer by using the time domain method, presented in the paper of Zhang et el [12], which allows significantly lower measurement uncertainty. The average ACS is determined from the average chamber time constants:

$$\langle \sigma_a \rangle = \frac{V}{c}\left(\frac{1}{\langle \tau_{wo} \rangle} - \frac{1}{\langle \tau_{no} \rangle}\right) \quad (5)$$

where V is the chamber volume, c is the velocity of light, $\langle \tau_{wo} \rangle$ and $\langle \tau_{no} \rangle$ are the average chamber power time constants with and without the object respectively. This method also has the advantage of being independent of the efficiency of the antennas used for the measurement.

The chamber time constant is obtained by applying the non-linear curve fitting technique described in [13] to the average power delay profile (PDP) of the input energy at each frequency of interest. The PDP is given by:

$$PDP(f_0) = \left\langle \left| IFFT\left[S_{21}(f,n) \cdot \mathrm{win}(f - f_0)\right] \right|^2 \right\rangle \quad (6)$$

where $S_{21}(f,n)$ is the transmission coefficient between the transmitting and receiving antennas at frequency f and stirrer position n; IFFT is the inverse fast Fourier transform operation; $\mathrm{win}(f - f_0)$ is a window function which selects a suitable band of frequencies about the desired frequency of interest f_0; and $\langle\ \rangle$ indicates an average over all the stirrer positions. In [12], Zhang et al described how to estimate the measurement uncertainty. By using the Monte Carlo method, the uncertainty of the measured ACS is calculated to be approximately 1%.

As the time domain method requires very small frequency steps to obtain a sufficiently long time-span in the IFFT, a segmented frequency sweeping technique was used; instead of sweeping the entire frequency band, only a narrow band around each frequency of interest is considered. In this way, the amount of data collected and the measurement time can be optimized. The distribution of frequency segments, which is depicted in Figure 4. A total of 171 segments are uniformly distributed from 1GHz to 18GHz. Each segment has a bandwidth of 5MHz and contains 51 equal-spaced points. In this paper we used a raised cosine window function. The continuous stirring technique was used and 800 stirrer positions were sampled at each frequency.

D. Powered and unpowered measurements

According to (2) and (5), for both frequency and time domain methods, two measurements are required to obtain the ACS. First the net power transfer function or the time constant of the empty chamber was measured, followed by that of the chamber loaded by the computer. The ACS of the unpowered and powered computer were each measured three times. When the computer was powered, the Windows 7 operating system was activated. To make the computer run at full capacity, a stress test program, HeavyLoad, was used [14]. It tests the CPU, GPU and hard drive simultaneously. In addition, a music CD was played by using the Windows media player to make full use of the CD-ROM. During all measurements the antennas and the computer were kept at the same places in the chamber. The only thing that changed was the power state of the computer.

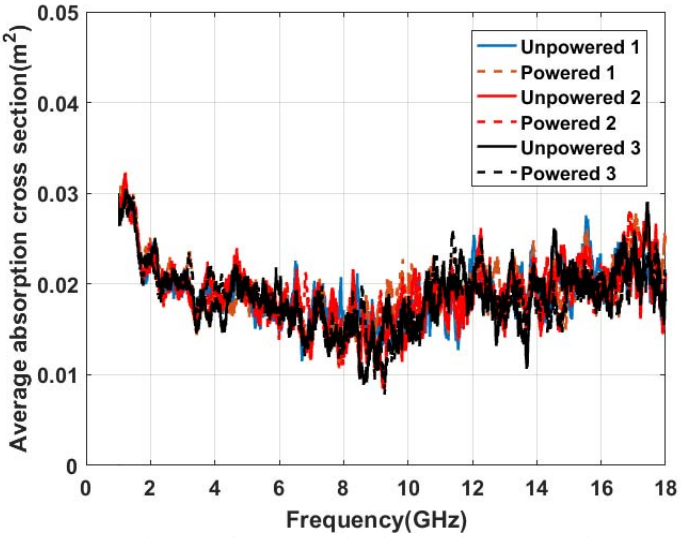

Fig. 5. Measured ACS of the unpowered and powered computer in the reverberation chamber (obtained by the frequency domain method)

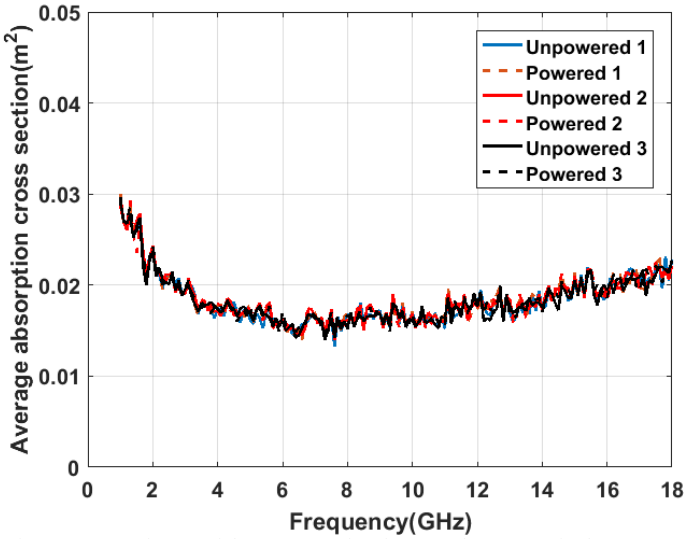

Fig. 6. Measured ACS of the unpowered and powered computer in the reverberation chamber (obtained by the time domain method)

IV. Results

Figure 5 shows the ACS of the unpowered and powered computer measured in the reverberation chamber by using the frequency domain method. It can be seen that the ACS of the computer has a value near 0.02m^2 over the whole frequency range. It is apparent that the measured ACSs of the computer are similar despite of different power states. Although they are not identical, the general features are the same. Whilst it is difficult to tell if there is any small difference in ACS between the powered and unpowered states, any difference that does exist is less than the ~20% statistical variation in the measurements.

As has been mentioned, the frequency domain method gives a relatively large measurement variability; therefore we decided to repeat the measurements with increased accuracy using the time-domain method. Figure 6 presents the measured ACSs of the unpowered and powered computer obtained by using the time domain method. It can be seen that the ACS of the computer is about 0.02 m^2, which is similar to the results obtained by the frequency domain method. Here we can see that any variation in ACS between powered and unpowered states is not obvious within the measurement uncertainty, which is ~1%.

Figure 7 shows a comparison between the ACS of the computer obtained by both frequency and time domain methods. The results shown in Figure 7 are the averages of the six measurements presented in Figure 5 and 6 respectively. It can be seen that both methods led to similar ACS. The time domain method has much lower measurement uncertainty than the frequency method. Ideally, for the frequency domain method, increasing the number of stirrer positions would reduce measurement uncertainty, but that would greatly increase the time of measurement. In this study, for instance, the frequency domain method took about

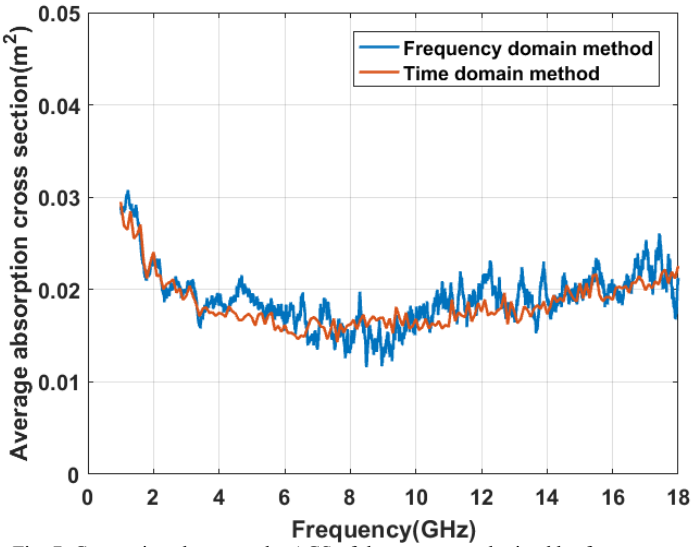

Fig. 7. Comparison between the ACS of the computer obtained by frequency and time domain methods.

40 minutes to finish 100 stirrer positions while the time domain method used only 10 minutes to finish 800 positions. Also the time domain method does not require the knowledge of the antenna efficiency. For the frequency domain method we allowed for the antenna reflection loss in (3) but on any loss within the antenna. However the antennas used have very low internal loss, so the ACSs measured by the two techniques are close.

V. Conclusions

In this paper we have presented results demonstrating how power state affects the ACS of electronic equipment. The ACS of a personal computer at different power states has been measured in a reverberation chamber over the frequency range of 1GHz to 18GHz by using both frequency

and time domain methods. The results suggest that for this computer, power state has little influence on its ACS.

Therefore, it can be concluded that for this computer, the ACS varies slowly with frequency and is independent of power state within 1% measurement variability. When performing similar ACS measurements in the future, there will be no need to consider power state, which will bring convenience to the measurements.

REFERENCES

[1] IEEE Standard Method for Measuring the Shielding Effectiveness of Enclosures and Boxes Having all Dimensions between 0.1 m and 2 m , IEEE Std 299.1-2013, 2014.

[2] D. W. P. Thomas, A. C. Denton, T. Konefal, T. Bensen, C. Christopoulos, J. F. Dawson, A. C. Marvin, S. J. Porter and P. Sewell, "Model of the electromagnetic fields inside a cuboidal enclosure populated with conducting planes or printed circuit boards" , IEEE Transactions on Electromagnetic Compatibility , vol. 43, no. 2 , pp. 161-169 , May 2001.

[3] A. C. Marvin, J. F. Dawson, S. Ward, L. Dawson, J. Clegg and A. Weissenfeld, "A proposed new definition and measurement of the shielding effect of equipment enclosures," IEEE Transcations on Electromagnetic Compatibility, vol. 46, no. 3, pp. 459-468, August 2004.

[4] A. Rusieski, K. Aniserowicz, A. P. Duffy and A. Orlandi, "Internal stirring: an approach to approximate evaluation of shielding effectiveness of small slotted enclosures," IET Science, Measurement Technology , vol. 10, no. 6 , pp. 659-664 , August 2016.

[5] S. L. Parker, I. D. Flintoft, A. C. Marvin, J.F Dawson, S.J. Bale, M. P. Robinson, M. Ye, C. Wan and M. Zhang "Predicting shielding effectiveness of populated enclosures using absorption cross section of PCBs," Proceedings of the 2016 International Symposium on Electromagnetic Compatibility, pp. 324-328, September 2016.

[6] D. A. Hill, M. T. Ma, A. R. Ondrejka, B. F. Riddle, M.L. Crawford and R. T. Johnk, "Aperture excitation of electrically large, lossy cavities," IEEE Transcations on Electromagnetic Compatibility, vol. 36, no. 3, pp. 169-178, August 1994.

[7] A. Gifuni, "Relation between the shielding effectiveness of an electrically large enclosure and the wall material under uniform and isotropic field conditions," IEEE Transcations on Electromagnetic Compatibility, vol. 55, no. 6, pp. 1354-1357, December 2013.

[8] I. D. Flintoft, S. L. Parker, S. J. Bale, A.C. Marvin, J. F. Dawson and M. P. Robinson, "Measured avergae abosrption cross-sections of printed circuit boards from 2 to 20 GHz," IEEE Transcations on Electromagnetic Compatibility, vol. 58, no. 2, pp. 553-560, April 2016.

[9] I. D. Flintoft, A. C. Marvin, M. P. Robinson, K. Fischer and A. J. Rowell, "The re-emission spectrum of digital hardware subjected to EMI," IEEE Transactions on Electromagnetic Compatibility , vol. 45, no. 4, pp. 576-585 , November 2003.

[10] I. D. Flintoft, S. J. Bale, S. L. Parker, A.C. Marvin, J. F. Dawson and M. P. Robinson, "On the measurable range of absorption cross section in a reverberation chamber," IEEE Transcations on Electromagnetic Compatibility, vol. 58, no. 1, pp. 22-29, February 2016.

[11] A. C. Marvin, G. Esposito, J. F. Dawson, I. D. Flintoft, L. Dawson, J. A. K. Everard and G. C. R. Melia, "A wide-band hybrid antenna for use in reverberation chambers," Proceedings of the 2013 International Symposium on Electromagnetic Compatibility, pp. 222-226, August 2013.

[12] X. Zhang, M. P. Robinson, I. D. Flintoft and J. F. Dawson, "Inverse Fourier transfer technique of measuring average absorption cross section in the reverberation chamber and Monte Carlo study of its uncertainty," Proceedings of the 2016 International Symposium on Electromagnetic Compatibility, pp. 263-267, September 2016.

[13] X. Zhang, M. Robinson and I. Flintoft, "On measurement of reverberation chamber time constant and related curve-fitting techniques," Proceedings of the 2015 International Symposium on Electromagnetic Compatibility, pp. 406-411, August 2015.

[14] HeavyLoad. [Online]. jam-software.com. Available: http://www.jam-software.com/heavyload. [Accessed: 14/10/2016].